NASA Contractor Report 198481

Compendium of Mechanical Limit-States

Michael Kowal
Vanderbilt University
Nashville, Tennessee

July 1996

Prepared for
Lewis Research Center
Under Grant NAG3–1352

National Aeronautics and
Space Administration

Table of Contents

Section

Introduction

Purpose

The creation of a compendium of mechanical limit states was undertaken in order to provide a reference base for the application of First-Order Reliability Methods to mechanical systems in the context of the development of a system level design methodology. The compendium was conceived as a reference source, specific to the problem of developing the noted design methodology, and not an exhaustive or exclusive compilation of mechanical limit states. The compendium is not intended to be a handbook of mechanical limit states for general use.

Proposed Use of Compendium

The compendium provides a diverse set of limit-state relationships for use in demonstrating the application of probabilistic reliability methods to mechanical systems. The different limit-state relationships will be used to analyze the reliability of a candidate mechanical system.

Selection of Limit-States

In determining the limit-states to be included in the compendium, a comprehensive listing of the possible failure modes that could affect mechanical systems was generated. Previous literature defining mechanical modes of failure was studied, and cited failure modes were included. From this, the following classifications for failure modes were derived:

- Wear
- Corrosion
- Fatigue
- Material Degradation

With the definition of the different failure modes, a literature search for each was conducted, with the aim of establishing relationships for each failure mechanism to be used in formulating mechanical limit-states.

The individual failure modes that were determined for each classification are:

Wear
- Adhesive wear
- Abrasive wear
- Lubricated wear
- Fretting wear
- Surface fatigue wear
- Liquid impact erosion

Corrosion
- Erosion-corrosion
- Galvanic corrosion
- Uniform attack
- Pitting corrosion
- Cavitation
- Crevice corrosion
- Stress corrosion cracking
- Selective leaching
- Inter-granular corrosion

Fatigue
- Low-cycle fatigue
- High-cycle fatigue
- Crack growth

Material Degradation
- Thermal degradation
- Radiation damage

Although it was possible to determine the different failure modes that could affect a mechanical system, the identification of relationships for all noted failure modes was not possible. The difficulty in identifying some of the limit-state relationships is due to a lack of accurate analytical models. Consequently, the compendium consists of relationships for those failure modes for which reasonably robust relationships exist.

Distribution Properties

The compendium does not contain information on the distribution properties of the individual primitive variables. With the exception of fatigue and wear related primitive variables, little research was uncovered that dealt with the distribution properties of limit-state primitive variables. There is significant research available on the best estimates of variables values, and when appropriate some of these values have been included in the relevant sections. The lack of much information on the distribution properties of many primitive variables indicates the need for additional research efforts in this area.

Form of Limit-State Relationships

The result of the investigation into mechanical limit-states indicate that the vast majority of identified relationships are of the form of a power law. All the limit states cited within the compendium, with the exception of those for uniform attack and thermal degradation, take a power law form.

Future Updates

The present version of the compendium does not include space environmental factors as outlined in Structural & Mechanical Systems Long-Life Assurance Design Guidelines[1]. The integration of space environment factors will be included in the second version of this document.

---

[1] Structural & Mechanical Systems Long-Life Assurance Design Guidelines, SwRI Report No. 06-1998-3, Southwest Research Institute, January 6, 1989.

Section 1:Wear

Wear is the removal of material from solid surfaces as a result of mechanical action. In most cases the amount of the material removed from the surfaces is small in relation to the overall material mass of the components involved.

Wear processes have been identified to conform to four different forms. The four major forms of wear enumerate by Rabinowicz[1] are:

1. Adhesive wear;
2. Abrasive wear;
3. Corrosive wear;
4. Surface fatigue wear.

In addition to these four major wear processes, there are a number of minor processes that are often categorized as being a wear process.

Models for the following wear processes are presented in sections 1.1 through 1.5:

1. Adhesive wear
2. Abrasive wear
3. Lubricated wear
4. Fretting wear
5. Liquid impact erosion.

---

1 Rabinowicz, E., Friction and Wear of Material, J. Wiley, New York, 1965.

1.1 Adhesive Wear

Definition

"Adhesive wear occurs when two smooth bodies are slid over each other, and fragments are pulled off one surface to adhere to the other" (Rabinowicz, 1965). Once the fragments have been torn from their original surface and attached to the opposing surface, they may reattach to their original surface, or become loose fragments.

Limit-State Formulation

Experimental data indicates that there are three laws of adhesive wear, namely;

1. The amount of wear is generally directly proportional to the load L;
2. The amount of wear is generally proportional to the distance slid, x;
3. The amount of wear is generally inversely proportional to the hardness, p, of the surface being worn away.

Holm (1946) proposed that the volume worn away could be described by:

$$V = \frac{cLx}{p} \tag{1}$$

where c=material dependent nondimensional constant

Evidence for this relationship is mixed, with some result being very close to the predicted volumes and other being widely different. Archard (1953) presented a model of sliding which allows for the derivation of the above equation, while providing insight into the meaning of the constant, c. From his model we get the following model for the volume of material worn away through adhesive wear;

$$V = \frac{kLx}{3p} \tag{2}$$

where k=coefficient of wear
=probability of any junction forming a fragment

p=flow pressure of softer metal

As can be seen the difference in these equations is that we have replaced *c* with *k/3*. The only important requirement for the second equation to hold is that the volume of the fragment should be proportional to the cube of the junction diameter.

An alternative form of the second equation is:

$$V = \frac{kA_r x}{3} \tag{3}$$

where A_r *=actual area of contact*

Although knowledge of the volume worn is important, typically we are more interested in the depth of material worn away. The extension of the above relations to yield the depth of material worn away is given in the Wear Control Handbook (ASME, 1980);

$$\frac{d}{L} = \frac{K P}{H}$$

where d=depth of wear
P=nominal pressure
L=sliding distance
H=material hardness

This form of the wear relationship now permits the estimation of the life of the surface. If we let the sliding distance, L, be expressed as the velocity, v, and the time, t, the relationship becomes:

$$t = \frac{d H}{K P v}$$

The authors go on to demonstrate that the coefficient of wear, K is the proportional of volume worn away to the theoretical worn volume that would have resulted if every asperity contact produced a worn particle.

Model Assumptions

The assumptions of the model are:

1. k=probability of any junction forming a fragment
2. Each junction is in existence throughout the sliding distance, d.

Notes

Values for k can be found in Proceedings of the Conference on Lubrication and Wear (1957 on), and the Transactions of the American Society of Lubrications Engineers (1958-1963).

Sources

Rabinowicz, E., Friction and Wear of Materials, J. Wiley, New York, 1965.

Holm, R., Electric Contacts, Almqvist and Wiksells, Stockholm, 1946.

Archard, J.F., *Contact and Rubbing of Flat Surfaces*, Journal of Applied Physics, vol. 24, pp.981-988.

Wear Control Handbook, ASME, 1980

1.2 Abrasive Wear

Definition

Abrasive wear occurs when a rough hard surface, or a soft surface containing hard particles, slides on a softer surface. As a result of the sliding action , the softer surface has a series of grooves ploughed into its surface. The material removed in the creation of the grooves is typically found to be loose particles.

Limit-State Formulation

Rabinowicz (1965), assuming that the hard surface was composed of conical asperities, derived the following relationship:

$$\frac{\partial V}{\partial l} = \frac{L\tan\theta}{\Pi p} \qquad (1)$$

where $\tan\theta$ *=weighted average angle of conical asperities*

This equation has the same form as the equation derived for adhesive wear. Thus we can use the same relationship as that for adhesive wear with the following value of the coefficient of wear:

$$k_{abr}=0.96 \tan\theta$$

Sources

See sources listed for adhesive wear.

1.3 Lubricated Wear

Definition

Lubricated wear occurs when two smooth surfaces are slid over each other in the presence of a lubricating media. The lubricating media serves to partially or completely separate the surface asperities of the opposing surfaces, thereby reducing or eliminating the formation of worn particles.

Failure Mechanism

Lubricated wear occurs when the degree of lubricant separating the two surfaces is insufficient to prevent asperity contact. If asperity contact occurs, then other wear mechanisms can be used to determine the wear.

Even under dry conditions, absorbed gas molecules act as a lubricant, thereby yielding less wear than predicted by theoretical relationships. A more accurate form of the standard wear relationship was offered by Rowe (Wear Control Handbook, p.143):

$$\frac{V}{d} = k_m A_m = k_m \alpha A = k_m \alpha \frac{L}{H}$$

where k_m = *adhesive wear coefficient free of contaminants*
A_m = *area of metallic contact*
α = *fraction of true area which is metal to metal*

Rowe then demonstrated:

$$\alpha = \frac{X}{U\, t_o} e^{-\frac{E}{RT_s}}$$

where X = *diameter of area of absorbed lubricant molecule*
t_o = *fundamental time of vibration of molecule in absorbed state*
U = *sliding velocity*
E = *energy of absorption*
T_s = *surface temperature*

The temperature rise in the contact surface can be approximated by:

$$\Delta T = \frac{gfWU}{8JK_{tc}r}$$

where g = *gravitational constant*
J = *mechanical equivalent of heat*
K_{tc} = *thermal conductivity*
f = *coefficient of friction*
r = *radius of contact area*

When wear particles begin to interact they breakdown the lubricant film and increase lubricant temperature. The result is collapse of lubricant film and catastrophic wear. This transition is marked by the end of mild wear processes, and the move to insufficient lubrication and catastrophic wear.

$$\frac{L}{U} = \frac{H\, t_o\, V}{K_m\, X\, d}\, e^{\frac{E}{RT_s}}$$

If it is assumed that,

$$\frac{V}{d} = \textit{Constant at onset of transition}$$

Then,

$$\left(\frac{L}{U}\right)_T = C\, e^{\frac{B}{T_T}}$$

where:
C, B *are constants*
T = *transition load-speed ratio and temperature*

The temperature rise in the contact surface can be approximated by:

$$\Delta T = \frac{gfWU}{8JK_{tc}r}$$

where g = *gravitational constant*
J = *mechanical equivalent of heat*
K_{tc} = *thermal conductivity*
f = *coefficient of friction*
r = *radius of contact area*

When wear particles begin to interact they breakdown the lubricant film and increase lubricant temperature. The result is collapse of lubricant film and catastrophic wear. This transition is marked by the end of mild wear processes, and the move to insufficient lubrication and catastrophic wear.

$$\frac{L}{U} = \frac{H\, t_o\, V}{K_m\, X\, d}\, e^{\frac{E}{RT_s}}$$

If it is assumed that,

$$\frac{V}{d} = \textit{Constant at onset of transition}$$

Then,

$$\left(\frac{L}{U}\right)_T = C\, e^{\frac{B}{T_T}}$$

where:
C, B *are constants*
T = *transition load-speed ratio and temperature*

Sources

See those sources listed for adhesive wear.

1.4 Fretting Wear

Definition

Fretting wear is the removal of material at a component interface that is the result of relative movement of the components, usually of such small magnitude that the movement is not detected by visual inspection.

Failure Mechanism

Fretting wear involves 3 possible basic processes:

1. Mechanical action disrupts oxide films on the surface exposing clean and possibly strained metal, which would be reactive and in atmosphere would oxidize rapidlyduring the colf cycle after disruption.

2. Removal of metal particles from the surface in a finely divided form by a mechanical grinding action or by formatio of welds at points of contact which are broken at a surface other thatn the original interface by shearing or fatigue.

3. Oxide debris resulting from either process 1, or 2 is an abrasive powder that damages the surfaces[1].

In observation of fretting behavior, research has found that:

1. Fretting damage is reduced in a vacuum or inert atmosphere.

2. Debris formed be fretting of iron is largely composed of Fe_2O_3.

3. Greater damage occurs at low frequencies for a given number of cycles compared with high frequencies.

4. Metal loss increases with load and relative slip.

5. Greater damage occurs below room temperature compared with above room temperature.

6. Damage is greater in dry atmospheric conditions than humid atmospheric conditions.[2]

Uhlig (1954) proposed a model of a regular array of asperities removed by successuve cycles. It is assumed that the asperities plough in the metal surfaces. From this a model for the weigth loss per cycle due to scraping of the oxide film layer was determined as:

---

[1] Waterhouse, R.B., *Fretting Corrosion*, Pergammon Press, London, 1972.

[2] Waterhouse, R.B., *Fretting Corrosion*

$$W_{CORR}=2nlck\ \ln\left(\frac{s}{2l\,f\,\tau}+1\right)$$

where: n=number of circular asperities/unit area
l=distance moved by an asperity in 1/2 cycle
=amplitude of slip
c=diameter of asperity
s=spacing of asperity
f=frequency
τ, k=constants

The weight loss per cycle due to the ploughing action is:

$$W_{MECH}=\frac{2k'lp}{p_o}=k_2lP$$

where: P=normal load
p_o=yield pressure
k', k_2=constants

Uhlig assumes a linear oxidation rate, so:

$$W_{CORR}=\frac{ncks}{f\,\tau}$$

Note that:
asperity spacing=$n^{0.5}$
total are of contact=$n\pi\ (c/2)^2$

Thus,

$$W_{CORR}=k_o\frac{P^{0.5}}{f}-k_1\frac{P}{f}$$

where: $k_o=\dfrac{2\ k}{\tau\ \sqrt{p_o\pi}}$

$$k_1=\frac{4\ k}{\tau\ p_o\pi}$$

Combining these results yields,

$$W_{TOTAL}=\frac{(k_o P^{0.5}-k_1 P)N}{f}+k_2\ IPN$$

where:N=total number of cycles

The previous relationships apply to the initial fretting which causes a fatigue crack and ultimately causes a fretting fatigue failure. The following notation will be used:

S_{MAX}	=maximum shear stress on asperities of bridge
p	=normal pressure on asperities
μ	=coefficient of friction
p_o	=yield pressure of weaker material
H	=hardness of bridge material
S_{alt}	=alternating shear stress in material due to alternating bending stress and frictional shear stress
σ_{alt}	=alternating bending stress in material
σ_y	=yield strength of weaker material

Assuming that:

i. $p_o=3\sigma_y$

ii. $\sigma_y=k\ H$

Assuming that the asperity contact is subjected to a shear stress, μp, then the maximum pressure that the asperity on the bridge can sustain is:

$$p=\frac{k_1\ H^2}{k_2+4\mu^2}$$

Small elements of the material experience alternating shear stress as a result of the alternating motion, the maximum value of which is :

$$S_{alt}=0.5\left(4\mu^2 p^2+\sigma_{alt}^2\right)^{0.5}$$

When the alternating shear stress, S_{alt}, reaches the fatigue strength of the material in shear, a fatigue crack will be initiated. The bending stress that will yield this critical value of the alternating shear stress is:

$$\sigma_{alt}=\left(4S_{alt}^2-\frac{4k_1\ H^2}{k_2+4\mu^2}\right)^{0.5}$$

Sources

Waterhouse, R.B., Fretting Corrosion, Pergammon Press, London, 1972.

Rabinowicz, E., Friction and Wear of Materials, J. Wiley, New York, 1965.

Wear Control Handbook, ASME, 1980.

1.5 Liquid Impact Erosion

Definition

Liquid impact erosion occurs when the action of a liquid striking a solid object results in the removal of the surface material.

Failure Mechanism

There are several models for liquid impact erosion, namely:

Thiruvengadam's Theory
Springer's Theory
Hertzian Theory
Evan's Elastic Plastic Theory

Each of these theories is discussed below.

Thiruvengadam's Theory of Liquid Impact Erosion

Thiruvengadam developed the notion of erosion strength, S_e.

S_e=energy absorbing capacity of material per unit volume under erosive forces.

The erosion process is controlled by 2 opposing phenomena:

1. time-dependent efficiency of absorption of impact energy by the material;
2. attentuation of impact pressure due to changing surface topography as the surface material is eroded.

The intensity of a single drop impact is defined as,

$$I_c = \frac{P_w^2}{\rho_w C_w}$$

where I_c=*intensity of impact*
P_w=*pressure imparted to surface by liquid impact*
ρ_w=*density of liquid*
C_w=*compressional wave velocity for liquid*

The attentuation of the intensity of impact, I_i, is assumed to be:

$$I_i=\left(\frac{A}{R+R_f}\right)^m I_e$$

where: I_i=attenuated intensity
A=proportionality constant
R=mean depth of erosion from original surface
R_f=thickness of liquid layer on surface

The intensity of erosion, defined as the power absorbed by a unit eroded area of material, is designated, I_e:

$$I_e=S_e\frac{dR}{dT}$$

and
$I_e=n\ I_i$

where n+$n(t)$ is time dependent property governing energy absorption efficiency.

This can be constructed into a normalized differential equation, the solution to which is;

$$\bar{\tau}=\frac{n}{\left(1+\bar{k}\frac{n+1}{n}\int_1^{\tau}\bar{n}d\tau\right)^{\frac{n}{n+1}}}$$

This approach has 2 weaknesses:

1. The dependence on the presence of a liquid layer on the surface to attenuate the loading pulses.
2. The parameter, n, is related to the theory, but has no physical meaning in most liquid drop situations, since the liquid layer is either thin or nonexistant.

Springer's Theory of Liquid Impact Erosion

Springer's theory is based on concepts involving metal fatigue. The model assumes that the incubation period, the acceleration period and the maximum rate period of the characteristic erosion curve can be represented by:

$$M^*=\alpha^*(N^*-N_i^*)$$

where: M^*=erosion mass loss
α^*=rate of mass loss
N^*=number of impacts per site
N_i^*=number of impacts corresponding to the incubation period

Based on Miner's rule in torsion and bending fatigue, Springer derives the expression for impacts in the incubation model:

$$N_I^* = a_1\left(\frac{S}{P}\right)^{a_2}$$

where: a_1, a_2 = *constants*
P = *avg. interfacial pressure due to water drop impact*

and

$$S = \frac{4\sigma_u(b-1)}{(1-2\nu)\left[1-(\sigma_{lower}\sigma_u)^{[b-1]}\right]}$$

where: ν = *Poisson's ratio*
σ_u = *ultimate tensile strength*
σ_l = *endurance limit*

$$b = \frac{b_2}{\log_{10}\left(\frac{\sigma_u}{\sigma_l}\right)} = \textit{derived from S-N curve}$$

From a least square fits of the data, $a_1 = 7 \times 10^{-6}$, and $a_2 = 5.7$.

The weakness of this approach is the arbitrary selection of a constant, b, which is applied to all materials.

Hertzian Impact Theory

In a collision of a deformable sphere and target, the time dependent radius of contact area is:

$$a(t) = a_1 \sin^{\frac{1}{2}} \left(\frac{\pi t}{T}\right)$$

where: $a_1 = K^{0.2} r\, v_0^{0.4}$ = *maximum contact radius*

$T = 2.943 K^{0.4} r\, v_0$ = *duration of bodies in contact*

$K = 1.25\pi \rho_1 \left[\frac{1}{\rho_1 C_1^2} + \frac{1}{\rho_2 C_2^2}\right]$ = *elastic properties of impacting bodies*

ρ_1, ρ_2 = *density of sphere and target*

C_1, C_2 = *elastic wave velocity of sphere and target*

$C_i^2 = \frac{1}{\rho_i} \frac{E}{(1-\nu^2)}$

If the liquid is assumed to be a deformable sphere impacting a rigid body, then when the relative velocity between the 2 bodies is 0,

$$a(t) = a_1 = \frac{5}{4}\pi^{0.2}\, r \left(\frac{V_o}{C_1}\right)^{0.4}$$

Zero relative velocity between the 2 bodies occurs at t=T/2.

The magnitude of the liquid impact pressure differs from those of solids, so the following results from the case of water hammer are used:

$$P_w = \rho_w\, C_w\, V_0$$

where: ρ_w = *density of liquid*

C_w = *acoustic wave velocity in liquid*

V_0 = *liquid impact velocity*

Accounting for the compressibility of the liquid,

$$P_w = \frac{\rho_w\, C_w\, V_0}{1 + \frac{\rho_w\, C_w}{\rho_t\, C_t}}$$

where the subscript ,t, denotes the properties of the target.

The impact of a water drop on a rigid surface was found by Engels to be:

$$P_w = \frac{\alpha}{2} \rho_w C_w v_0$$

Evans' Elastic-Plastic Theory

Evans proposes that the predicted erosion rate is:

$$V = v_0^{\frac{19}{6}} \; r_{\frac{11}{3}} \; \rho^{\frac{19}{12}} \; Ke^{\frac{-4}{3}} \; H^{\frac{-1}{4}}$$

where: V = *volume lost/impact*
v_0 = *impact velocity*
r = *particle radius*
ρ = *particle density*
Ke = *stress intensity factor*
H = *dynamic hardness*

Sources

Wear Control Handbook, ASME, 1980

Section 2:Corrosion

Corrosion is the destructive attack of a metal by chemical or electrochemical reaction with it environment.[1] The destruction of a metal surface by physical causes is not classified as corrosion.

The major classifications of corrosion given by Fontana[2] are:

1. Erosion-corrosion
2. Galvanic corrosion
3. Uniform attack
4. Pitting corrosion
5. Cavitation
6. Crevice corrosion
7. Stress corrosion cracking
8. Selective leaching
9. Intergranular corrosion

Models for the first six forms of corrosion were found, and are presented in sections 2.1 through 2.6 that follow. At this time no deterministic relationships were found that accurately predict stress corrosion cracking, selective leaching, or intergranular corrosion.

---

[1] Uhlig, H., Corrosion and Corrosion Control, 2nd Edition, p.1, J. Wiley & Sons Inc., 1971.

[2] Fontana, M., Corrosion Engineering, Third Edition, McGraw-Hill Book Co., San Francisco, 1986.

2.1 Erosion-Corrosion

Definition

Erosion-corrosion is defined as the accelerated corrosion of a metal as a result of a flowing fluid disrupting or thinning a protective film of corrosion products.

Failure Mechanism

The transition from laminar to turbulent flow occurs over a velocity range and is dependent on the geometry, surface roughness, and liquid viscosity. The conditions of fluid flow and the transition to turbulent flow is predicted using the Reynolds number:

$$Re = \frac{V\,d}{\gamma}$$

where: V = velocity($m\ s^{-1}$)
d = characteristic specimen length (m)
γ = kinematic viscosity ($m^2\ s$-1)

When a liquid exhibits predominantly turbulent flow, a thin laminar sublayer, of thickness δh, exists near the metal surface as a result of viscous drag. If material is being removed from the metal surface the will be a diffusional boundary layer of thickness δd.[1] The Schmidt number describes the relationship between these two boundary layers:

$$Sc = \frac{\gamma}{D}$$

where: D = diffusivity of the relevant species (m/s)

As the value of the Schmidt number increases the diffusion layer will become thinner, and its formation occur more rapidly.[2]

In most cases the resistance of the surface to mass transfer, both laminar and turbulent regions of flow, is accomplished through the definition of the mass transfer coefficient, K , as:

$$K = \frac{\text{rate of reaction}}{\text{concentration driving force}}$$

---

1 Poulson, B., *Electrochemical Measurements in Flowing Solutions*, Corrosion Science, vol. 23, no. 4, pp.391-430, 1983.

2 Poulson, B., *Electrochemical Measurements in Flowing Solutions*

The mass transfer rate is more conveniently described by a dimensionless number, the Sherwood number,

$$Sh=\frac{K\,d}{D}$$

For reactions that are governed by mass transfer, the relationship between the Sherwood, Reynolds, and the Schmidt numbers is found by empirical results to be of the form,

$$Sh=constant\cdot Re^{x}\cdot Sc^{y}$$

Typical experimental results indicate that x is usually 0.3-1, and y is 0.33. These values are applicable in cases where the surface is initially smooth. The case of rough surfaces subjected to mass transfer is outlined below. In addition, the consideration of different surface configurations that may be subject to erosion-corrosion is accommodated by the constant in the above equation, a constant that is geometry dependent. The most common geometries studied, and some results are outlined in the next section.

When a metal is subjected to erosion corrosion it will develop scallop shaped ridges. The roughening due to the creation of these ridges tends to increase the mass transfer rate, and the rate of erosion corrosion. The availability of relationships defining either mass transfer or erosion corrosion from rough surfaces is extremely limited. Recent work has indicated that once a surface is roughened, the rate of mass transfer is governed by roughness, not the geometry of the surface[3]. More importantly, the results indicate that a universal governing relationship for mass transfer for roughened surfaces may exist, namely,

$$Sh=0.01\ Re\ Sc^{0.33}$$

The results indicating such a result are shown in Figure 1, taken from Poulson (Corr. Sc., 1990). Poulson does indicate that the main differences between geometries is their tendency to roughen; he cites that bends in pipes tend to roughen faster, probably as a result of their attaining a critical Reynolds number more easily. Although the smooth surface mass transfer relationships are useful for the prediction of initial rates of erosion corrosion, the roughened surface relationship will govern the erosion corrosion process once the surface is no longer smooth. The precise point at which the roughened surface relationship is applicable has yet to be established.

---

[3] Poulson, B., *Mass Transfer From Rough Surfaces*, Corrosion Science, vol. 30, no. 6/7, pp.743-746, 1990

Sources

Abdulsalam, M., and J.T. Stanley, *Steady-State Model for Erosion-Corrosion of Feedwater Piping*, Corrosion, vol. 48, no. 7, pp.587-593, 1992.

Heitz, E., *Chemo-Mechanical Effects of Flow on Corrosion*, Corrosion Engineering, vol. 47, no.2, pp. 135-145, 1991.

Kappesser, R., I. Cornet, and R.Greif, *Mass Transfer to a Rough Rotating Cylinder*, Electrochemical Science, Dec., 1971, pp. 1957-1959.

Markin, A.N., I.S. Sivokin, and A.G. Khurshudov, *Mathematical Simulation of Corrosion-Electrochemical Processes*, Corrosion, vol. 47, no.9, pp.659-664, 1991.

Nesic, S., and J. Postlethewaite, *Relationship Between the Structure of Disturbed Flow and Erosion-Corrosion*, Corrosion, vol. 46, no. 11, pp.874-880, 1990.

Nesic, S., and J. Postlethwaite, *A Predictive Model for Localized Erosion-Corrosion*, Corrosion, vol. 47, no. 8, pp.582-589, 1991.

Nesic, S., and J. Postlethwaite, *Hydrodynamics of Disturbed Flow and Erosion-Corrosion:Part I-Single-phase Flow Study*, Canadian Journal of Chemical Engineering, vol. 69, pp.698-710, June, 1991.

Postlethwaite, J., M.H. Dobbin, and K. Bergevin, *The Role of Oxygen Mass Transfer in the Erosion-Corrosion of Slurry Pipelines*, Corrosion, vol. 42, no. 9, pp.514-521, 1986.

Postlethwaite, J., and U. Lotz, *Mass Transfer at Erosion-Corrosion Roughened Surfaces*, Canadian Journal of Chemical Engineering, vol. 66, pp. 75-78, Feb., 1988.

Poulson, B., *Electrochemical Measurements in Flowing Solutions*, Corrosion Science, vol. 23, no. 4, pp.391-430, 1983.

Poulson, B., and R. Robinson, *The Use of a Corrosion Process to Obtain Mass Transfer Data*, Corrosion Science, vol. 26, no. 4, pp. 265-280, 1986.

Poulson, B., *Mass Transfer From Rough Surfaces*, Corrosion Science, vol. 30, no. 6/7, pp.743-746, 1990.

Symbol	Geometry	Technique	Equation	Ref
∩	2·5d 180° bend in 22·6mm tube	copper in ·1N HCl+4g/l Fe^{3+}	$Sh=\cdot 01 Re^{\cdot 98} Sc^{\cdot 33}$	16
⊥	95mm impinging jet at height 95mm		$Sh=\cdot 065 Re^{1\cdot 02} Sc^{\cdot 33}$	17
▫	rotating cyclinder $\frac{d}{\epsilon}=87$	LCDT	$Sh=\cdot 016 Re^{\cdot 95} Sc^{\cdot 33}$	10
●	90mm pipe	plaster dissolution	$Sh=\cdot 02 Re^{\cdot 9} Sc^{\cdot 33}$	13

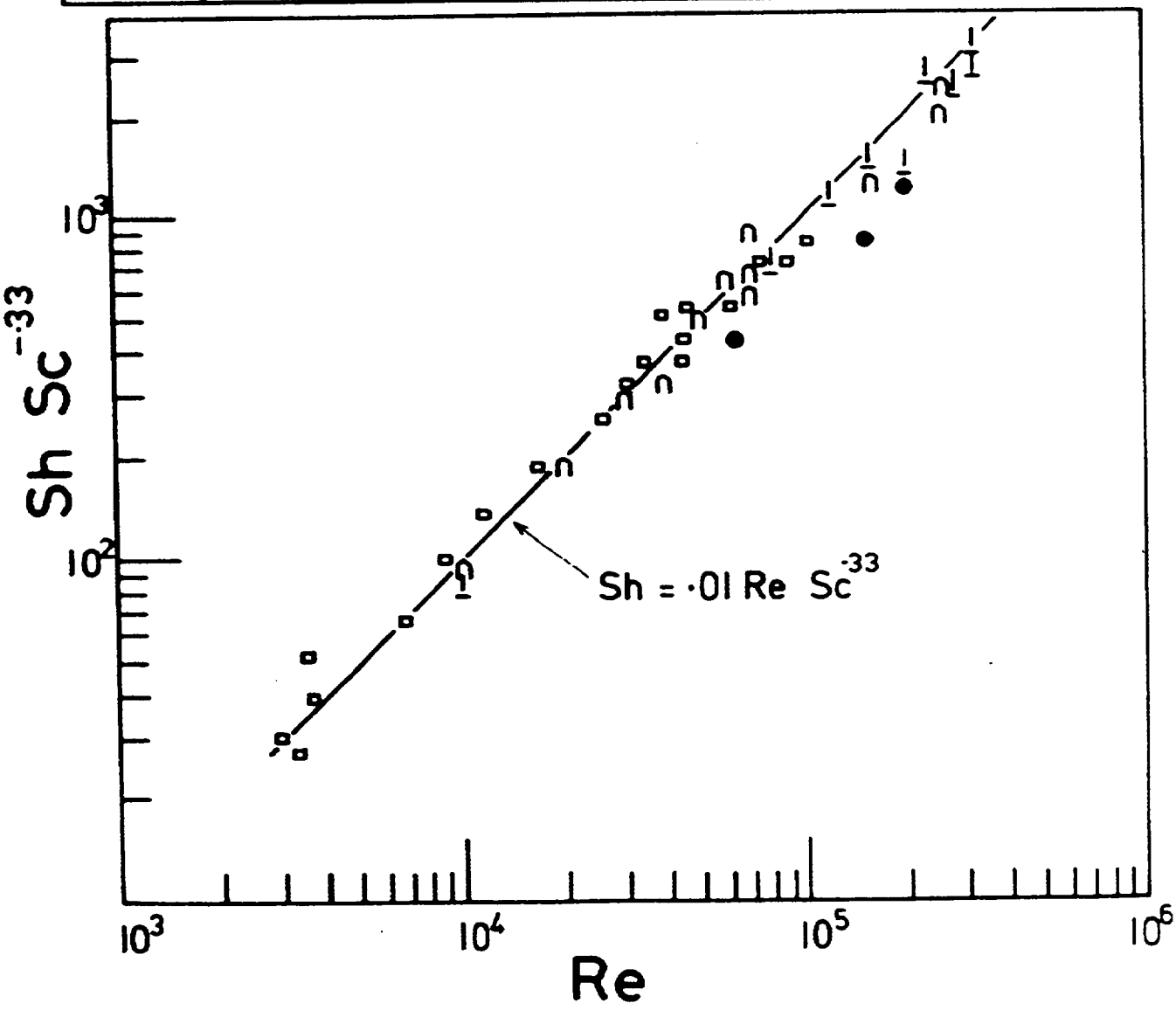

FIG 1 MASS TRANSFER FROM ROUGH SURFACES

Initial Erosion Corrosion Geometry-Dependent Relationships

The following table gives the initial smooth surface erosion corrosion rates.
(From Poulson, B., *Electrochemical Measurements in Flowing Solutions*, Corrosion Science, vol. 23, no. 4, pp. 391-430, 1983)

ROTATING DISC	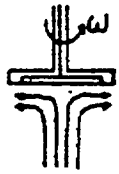	$Re = \frac{\omega r^2}{\nu}$ $Re_c = 1.7 \cdot 35 \times 10^5$	$\overline{Sh}_L = 0.620\ Re^{.5}\ Sc^{.33}$ $\overline{Sh}_T = 0.0078\ Re^{.9}\ Sc^{.33}$
ROTATING CYLINDER	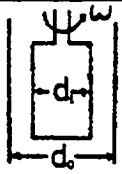	$Re = \frac{dV}{\nu} = \frac{\omega d_i^2}{2\nu}$ $Re_c \sim 200$	$\overline{Sh}_{smooth} = 0.079\ Re^{.7}\ Sc^{.356}$ $\overline{Sh}_{rough} = (1.25 + 5.76 \log_{10} d/\ell)^{.7}\ Re\ Sc^{.356}$
IMPINGING JET	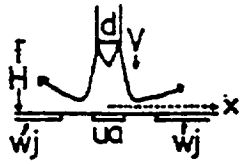	$Re = \frac{dV}{\nu}$ $Re_c \cong 2000$	$\overline{Sh}_{WA} = 1.12 \cdot Re^{.5}\ Sc^{.33}\ (H/d)^{.051}$ $Sh_{WJ} = .65\ Re^{.64}\ (x/d)^{-1.2}$
NOZZLE OR ORIFICE	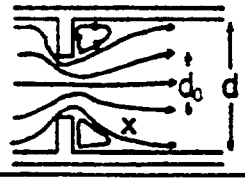	$Re_D = \frac{d_0 V_0}{\nu}$ $Re_c \sim 600$	$Sh_{MAX} = .276\ Re_0^{.46}\ Sc^{.33}$ $\frac{Sh_x}{Sh_{fd}} = 1 + A_x \left[1 + B_x \left(\frac{Re_0^{.46}}{.0165\ Re^{.46}} - 2\right)\right]$
TUBE	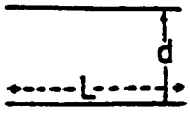	$Re = \frac{dV}{\nu}$ $Re_c \cong 2000$	$\overline{Sh}_L = 1.61 (Re\ Sc\ d/L)^{.33}$ $\overline{Sh}_T = .276\ Re^{.583} Sc^{.33} (d/L)^{.33}$ $\overline{Sh}_{fdT} = .0165\ Re^{.86}\ Sc^{.33}$

2.2 Galvanic Corrosion

Definition

Galvanic corrosion is the corrosion associated with the current of a galvanic cell made up of dissimilar electrodes.[1]

Failure Mechanism

The fundamental behavior of galvanic corrosion follows the behavior of a dry cell. The relationship between the current flow in a dry cell and the weight of material corroded is given by Faraday's law:

$$W = k\ I\ t$$

where: W = weight of metal reacting
k = electrochemical equivalent
I = current in amperes
t = time in seconds

It is important to distinguish between the open-circuit potential of a system and the corrosion potential of a system. The corrosion potential of the system is not the open-circuit potential of the system since the electrode reactions going on are continuously dissipating energy.

In determining the galvanic corrosion, the initial step is the establishment of the corrosion potential, ϕ_{corros}. The potential difference of the polarized electrodes, ϕ, is given by[2]:

$$\phi = I_1(R_e + R_m)$$

where: ϕ = potential difference
I_1 = current
R_e = electrolytic resistance
R_m = external metal resistance

On short circuit, the current becomes the maximum current, I_{MAX}, and R_M can be neglected, resulting in the potential difference being[3]:

$$\phi = I_{MAX} R_e$$

The measured potential of a corroding metal is the corrosion potential, ϕ_{corros}. The value of the

---

1 Uhlig, H., The Corrosion Handbook, J. Wiley & Sons, Inc., New York, 1948.

2 Uhlig, H., Corrosion and Corrosion Control, pp. 38-39.

3 Uhlig, H., Corrosion and Corrosion Control, p.39.

maximum current, I_{MAX}, is known as the corrosion current, I_{corros}. The corrosion rate of the anodic areas on a metal surface is related to I_{corros} by Faraday's Law.[4] By applying Faraday's Law, the corrosion rate per unit area can be expressed as a current density.

The potential of the system changes as the reaction progresses, resulting from net current to or from the electrode, and this process is referred to as polarization. The result is the system potential does not remain constant, resulting in variable current density. The are three causes of polarization[5]:

1.*Concentration Polarization*

Concentration polarization occurs when, as a result of the current flow, material is deposited on the electrode, decreasing the surface concentration of ions. Infinite concentration polarization is approached when the concentration of ions on the surface approaches zero. The corresponding current density is referred to the limiting current density. For conditions where concentration polarization is present, the difference in the material potentials is given by;

$$\phi_2-\phi_1=-\frac{RT}{nF}\ln\frac{i_L}{i_L-i}$$

where: $\phi_2-\phi_1$ *=difference ∈ potentials*
R=gas constant (8.314 *J/deg-mole*)
T=absolute temperature
*F=Faraday=*96500 *C/eq*
n=number of electrons involved in the reaction
i_L *=limiting current density*
i=applied current density

The limiting current density (A/cm^2) can be determined from:

$$i_L=\frac{DnF}{\delta t}c\ X\ 10^{-3}$$

where: D=diffusion coefficient for reduced ion
δ=thickness of the stagnant layer of electrolyte on electrode surface
t=transference number of all ions in solution except reduced ion
c=concentration of diffusing ion (moles/liter)

For all ions at 25°C, with the exception of H and OH, D averages about 1 X 10^{-5} cm^2/sec, and the limiting current density can be approximated by:

---

4 Uhlig, H., Corrosion and Corrosion Control, p. 39.

5 Uhlig, H., Corrosion and Corrosion Control, pp.42-47.

i_L=0.02 nc.

2.*Activation Polarization*

In this case, the polarization is the result of a slow electrode reaction; or equivalently, the electrode requires an activation energy in order to proceed[6]. The activation polarization, η, increases with the current density according to:

$$\eta = \beta \log \frac{i}{i_o}$$

Note that both β and η are constant for each metal and environment, and are temperature dependent. The exchange current, i_o, is the current density equivalent to the equal forward and reverse reactions at the electrode at equilibrium[7].

3.*IR Drop*

The polarization includes a drop in the potential for the electrolyte surrounding the electrode.

---

6 Uhlig, H., Corrosion and Corrosion Control, pp.44-46.

7 Uhlig, H., Corrosion and Corrosion Control, p.45.

Calculation of Corrosion Rates

In determining the corrosion rate, the anode-cathode area ratio must first be considered. If A_a is the fraction of the surface that is anode, and A_c is the fraction that is cathode, such that $A_a+A_c=1$, then:

$$\phi_c'=\phi_c-\beta_c \log\frac{I_c}{A_c i_{oc}}$$

$$\phi_a'=\phi_a+\beta_a \log\frac{I_a}{A_a i_{oc}}$$

where: ϕ_c' *= polarized potential-cathode*
ϕ_a' *= polarized potential-anode*
ϕ_c *= open-circuit potential-cathode*
ϕ_a *= open-circuit potential-anode*
β_c *= Tafel slope-cathode*
β_a *= Tafel slope-anode*
I *= current per unit metal surface area*

When the system is in steady state, $\phi'_c=\phi'_a=\phi_{corros}$, and $I_a=I_c=I_{corros}$, then the maximum corrosion current occurs when:

$$\beta_c(1-A_c)-\beta_c A_c=0$$

$$or\ A_c=\frac{\beta_c}{(\beta_c+\beta_a)}$$

If $\beta_c=\beta_a$, then the maximum corrosion rate occurs when $A_c=A_a=0.5$.

In estimating the corrosion current, if the solution is a dearated acid, then the following relationship is a useful approximation:

$$\phi_{corros}=-\left[0.059\ pH+\beta \log\frac{i_{corros}}{i_o}\right]$$

Alternatively, Stern and Geary[8], derived the following relationship:

$$I_{corros} = \frac{I_{applied}}{2.3\ \Delta\ \phi}\left(\frac{\beta_c \beta_a}{\beta_c + \beta_a}\right)$$

where: β_a = *Tafel constant for anodic reaction*

β_c = *Tafel constant for cathodic reaction*

$\frac{I_{applied}}{\Delta\ \phi}$ = *polarization slope in region near corrosion potential*

Once the corrosion current has been determined, the corrosion rate can be found using Faraday's Law.

Sources

Bockris, J., et al. ed., Comprehensive Treatise of Electrochemistry:Volume 4 Electrochemical Materials Science, Plenum Press, New York, 1981.

Makrides, A.C., and N. Hackerman, *Dissolution of Metals in Aqueous Acid Solutions*, J. Electrochemical Soc., vol. 105, no.3, pp.156-162, 1958.

Munn, R.S., and O.F. Devereux, *Numerical Modeling and Solution of Galvanic Corrosion Systems*, Corrosion, vol. 47, no. 8, pp. 612-634, 1991.

Uhlig, H., The Corrosion Handbook, J. Wiley & Sons, New York, 1948.

Uhlig, H., Corrosion and Corrosion Control, Second Edition, J. Wiley & Sons, New York, 1971.

[8] Stern, M., and A. Geary, *J. Electrochem. Soc.*, vol. 104, no. 56, 1958.

2.3 Uniform Attack

Definition

Uniform attack is the destruction of a material as a result of an electrochemical reaction with its environment, where the rate of corrosion is constant over the material surface.

Failure Mechanism

No empirical relationship exists to predict the rate of uniform attack of a material. Typically, materials are arranged into 3 categories of susceptibility to uniform attack (low, moderate, high), and little predictive work has been done.

Despite the few models available for uniform attack, the application of an Arrhenius type relationship would permit the prediction of rates of corrosion at differing temperatures and corrosive environments. The use of an Arrhenius relationship assumes that the corrosion rate is constant up to a critical temperature, T^C, and increasing rates of corrosion at temperatures in excess of T^C. In addition, the Arrhenius model assumes that the material is continually exposed to the corrosive environment, with the concentration of corrosives remaining fixed. The model is then:

For $T < T^C$

$$ML = C = Constant$$

For $T \leq T^C$

$$ML = Ce^{-\frac{\phi}{k}\left(\frac{1}{T^C}-\frac{1}{T}\right)}$$

where: ML = *rate of material loss (ipy)*
C = *constant corrosion rate:specific to material and environment*
ϕ = *activation energy for corrosion (eV)*
k = *Boltzmann constant* (0.8617×10^{-4} *eV/K*)
T = *absolute temperature of the environment* (° *K*)
T^C = *absolute temperature-critical* (° *K*)

The sum of the rates of material loss for each temperature exposure multiplied by the exposure duration should yield the total material loss.

Sources

Fontana, M., Corrosion Engineering, Third Edition, McGraw-Hill Book Co., San Francisco, 1986.

Uhlig, H., The Corrosion Handbook, J. Wiley & Sons, New York, 1948.

Corrosion, Volume 13, Metals Handbook, 9th ed., ASM International, Metals PArk, OH, 1987.

2.4 Pitting Corrosion

Definition

"Pitting corrosion is the local dissolution leading to the formation of cavities in passivated metals or alloys that are exposed to aqueous, nearly neutral solution containing aggressive anions."[1] Pitting corrosion is characterized by the fact that pitting will be not initiated if the anodic potential is below a critical threshold value.

Failure Mechanism

Pitting corrosion is dependent on three factors:

1. The anodic potential exceeding the critical potential for pit nucleation, E_{np}.
2. The time required to form the first pit on a passive metal exposed to a solution containing aggressive anions, referred to as the induction time for pit initiation, τ.
3. The kinetics of pit growth.

The induction time for pit initiation is inversely related to the concentration of chloride ions, Cl^-, or the potential. The induction time for pit initiation is thought to represent the time to penetrate the passive film. Studies by Nishimura and Kudo, and Knittel et al., demonstrated that τ was proportional to the thickness of the passive film barrier layer.

Pit induction time is greatly affected by the concentration of chloride ions in the solution; the relationship is given by:

$$\frac{1}{\tau} = k([Cl^-]-[Cl]^*)$$

where: $[Cl]^*$ = *critical* Cl^- *concentration (pitting if* $Cl^- > [Cl^-]^*$)

Hoar and Jacob (1967) determined τ for 18Cr-8Ni stainless steel. The rate of pit initiation, τ, was found to be proportional to the n^{th} power of the Cl^- concentration, for the region where n was between 2.5 to 4.5. Other researchers have determined the values of n for different materials (see attached table from Szklarska-Smialowska).

---

[1] Szklarska-Smialowska, Z., Pitting Corrosion of Metals, NACE, Houston, 1986.

The determination of pit growth is easy for the potentiostatic case. Szklarska-Smialowska[2] reported that Engell and Stolica found that the rate of pit growth was:

$$i=i^* + k_1 (t-\tau)^b$$

where: i=total current
i^*=current in passive state
t=total time
τ=induction time
k_1, b are constants

If the passive state current is disregarded and the time, t, is calculated from the beginning of the pit propagation, then the relationship becomes:

$$i=k \cdot t^b$$

In this case, k is dependent on the concentration of the chloride ion, Cl^-. If the number of pits is constant over time, then b=2; if the number of pits increases with time, then b=3. The assumptions made in this model are:

1. Pits are hemispherical in shape.

2. Current density in the pits is constant; thus the pit radii should increase linearly with time.

Szklarska-Smialowska[3] reported that Forchhammer and Engell studied the growth of the pit radius, r, and the number of pits, N, and found:

$$r=k \cdot t^{\frac{1}{3}}$$

In addition, the research found that the coefficient b, cited above, varied from 0.6 to 1.2 for austenitic stainless steels.

Godard[4] found that the greatest pit depth, d, in aluminum was proportional to:

$$d=k \cdot t^{\frac{1}{3}}$$

---

2 Szklarska-Smialowska, Z., Pitting Corrosion of Metals, p. 113.

3 Szklarska-Smialowska, Z., Pitting Corrosion of Metals, p. 115.

4 Godard, H.P., *Pitting Kinetics*, Canadian Journal of Chemical Engineering, vol. 21, p.167, 1960.

The results of numerous studies found that the relationship proposed for pit growth is not applicable in all situations. This led Szklarska-Smialowska to propose three models:

Case 1 Hemispherical Pit Model (r=h)

$$i \sim \frac{r^3}{t} N$$

Case 2 Cap Shaped Pit Model (r>h)

$$i \cong \frac{h^2 R(3-\alpha)}{t} N$$

Case 3 Cylinder Shaped Pit Model (r<h)

$$i \sim \frac{r^2 h}{t} N$$

Sources

Fontana, M., Corrosion Engineering, Third Edition, McGraw-Hill Book Co., San Francisco, 1986.

Godard, H.P., *Pitting Kinetics*, Canadian Journal of Chemical Engineering, vol. 21, p.167, 1960.

Szklarska-Smialowska, Z., Pitting Corrosion of Metals, NACE, Houston, 1986.

Uhlig, H., The Corrosion Handbook, J. Wiley & Sons, Inc., New York, 1948.

Order of Reaction Values, n.

(From Szklarska-Smialowska, Z., Pitting Corrosion of Metals, p. 110, 1986)

Metal or Alloy	Aggressive Anion	pH	n	Potential
Al 1199	low Cl^- conc.	0.0	11.1	0.18 V_{SCE}
	higher Cl^- conc.		4.0	
Al 2024	0.004-0.01M Cl^-	0.0	3.0	
(99.99% Al)	0.003-0.004M Cl^-	0.0	8.8	0.18 V_{SCE}
	(in H_2SO_4)	3.5	4.8	
Pure, preanodized	0.01-1M KCl	6.1	0.1	
Al	1-3M KCl	5.9-	0.9	
	Cl^-	0.3	8	
	Br^-	0.3	4	
Al alloy	I^-	0.3	2	0.18 V_{SCE}
7075	F^-	5.8	3	
	Cl^-	5.8	2	
	Br^-	5.8	2	
Al 1199	Cl^-	3.56	1.5	0.6 V_{Hg/Hg_2SO_4}
	Br^-	3.56	2.5	
18Cr-8Ni stainless	Cl^-	2.0	2.5-4.5	0.4-0.8 V_{SHE}
Iron	10^{-3}M Cl^- in H_2SO_4	0.0	3	0.85-1.75 V_{SHE}
Nickel	low Cl^- conc.	2.0	4	0.5 V_{SCE}
	high Cl^- conc. in H_2SO_4		3	
18Cr-8Ni stainless	Cl^- in H_2SO_4	0.0	2.5	0.2 V_{SCE}
			4.5-5	0.6 V_{SCE}

2.5 Cavitation

Definition

Cavitation is a dynamic phenomena that is concerned with the growth and collapse of cavities in a liquid. Cavitation is a liquid phenomena that is the result of pressure reductions in the liquid.

It is important to note that:

1. cavitation can occur in liquids in motion or at rest.

2. cavitation is not restricted to or excluded from occurring at solid boundaries.

Failure Mechanism

At this time no comprehensive model that adequately predicts the behavior of cavitation erosion is available. Existing models of cavitation erosion have focussed on extremely simplifed cases involving the collapse of singe cavities on a solid surface. The agreement between such models and experimentally observed results varies. This being the case, the best guide to the designer is the avoidance of situations where cavitation can occur.

The cavitation number, σ, is a useful parameter for categorizing cavitating flows and is defined as:

$$\sigma \equiv \frac{P_\infty - P_V}{0.5\ \rho\ V_\infty^2}$$

where: P_∞ = *absolute pressure at some reference locality*
P_V = *vapor pressure (at liquid bulk temperature)*
V_∞ = *reference velocity*
ρ = *liquid density*

If the value of σ is large, then no cavitation will occur, while if σ is sufficiently small then cavitation behavior will be well developed. Limited cavitation will occur when the cavitation number is of some intermediate value. This is exhibited by a few bubbles in the flow. The limited cavitation number which describes this state is:

$$\sigma_L \equiv \frac{P_{\infty L} - P_V}{0.5\ \rho\ V_\infty^2}$$

Here, $P_{\infty L}$ is the absolute pressure at the reference locality that corresponds to the state of limited cavitation.

The determination of the nature of cavitation has been studied with two different approaches:

1. *Desinent Cavitation*

   In this case cavitation is established while holding the velocity constant, and then increasing the pressure until the cavitation disappears at a pressure value, referred to as the desinence pressure, $P_{\infty d}$. The desinent cavitation number is determined from the same relation at that above, with the exception that P_{∞} is replaced by $P_{\infty d}$.

2. *Incipient Cavitation*

   In this case velocity is held constant, eliminating all cavitation, and then the pressure is decreased until cavitation appear at the inception pressure, $P_{\infty i}$. The incipient cavitation number is determinde by replacing P_{∞}, by $P_{\infty i}$ and applying the above relationships.

Sources

Holl, J.W., *Limited Cavitation*, Proceedings of the ASME Fluids Engineering and Applied Mechanics Conference, Northwestern University, Evanston, Illinois, June 16-18, 1969.

Knapp, R.T., J.W. Daily, and F.D. Hammitt, Cavitation , McGraw-Hill Book Co., New York, 1970.

2.6 Crevice Corrosion

Definition

"Crevice corrosion occurs when two or more surfaces in close proximity lead to the creation of a locally occluded region where enhanced dissolution can occur."[1] The rate of crevice corrosion is usually a function of the depth and width of the crevice. The distinction between crevice corrosion and pitting is that crevice corrosion proceeds at a much faster rate than pitting. This more rapid corrosion rate is a result of the restrictive crevice geometry which permits the crevice electrolytic solution to under change much more rapidly than a pit.

Failure Mechanism

The complex nature of crevice corrosion has made prediction of crevice corrosion rates difficult. At present, no accurate deterministic model of crevice corrosion exits. The current approach favored for the evaluation of crevice corrosion is the application of finite element methods. A number of packaged computer programs are available to predict crevice corrosion based on finite element methods, including:

CHEQMATE-CHemical EQuilibrium with Migration And Transport Equations developed by A. Haworth, S.M. Sharland, P.W. Tasker, and C.J. Tweed outlined in Harwell Laboratory Report, NSS-R113, 1988.

HARWELL-presented by C.P. Jackson, *The TSGL Finite-Element Subroutine Library*, AERE Report AERE-R10713, 1982.

---

[1] Sharland, S.M., *A Mathematical Model of the Initiation of Crevice Corrosion in Metals*, Corrosion Science, vol. 33, no. 2, p. 183, 1992.

Governing Equations

'The transportation of aqueous species i is governed by the mass-balance equation. The mass-balance equation describes the diffusion under concentration gradients, electromigration under potential gradients, and chemical reaction.'[2] The mass-balance equation is:

$$\frac{\partial C_i}{\partial t} = D_i \nabla^2 C_i + z_i U_i F \nabla(C_i \nabla \phi) + R_i$$

where: C_i = *concentration of species i*
D_i = *effective diffusion coefficient*
z_i = *charge number*
R_i = *rate of production/depletion of species i by chemical reaction*
U_i = *mobility* $= \frac{D_i}{RT}$

For a crevice geometry that is assumed to be rectangular, the steady-state transport equations for species i is:

$$D_i\left(\frac{\partial^2 C_i}{\partial x^2} + \frac{\partial^2 C_i}{\partial y^2}\right) + \frac{z_i D_i F}{RT}\left[\frac{\partial}{\partial x}\left(C_i \frac{\partial \phi}{\partial x}\right) + \frac{\partial}{\partial y}\left(C_i \frac{\partial \phi}{\partial y}\right)\right] + R_i = 0$$

The boundary conditions are usually then determined.

Sources

Bockris, J., et al. ed., Comprehensive Treatise of Electrochemistry:Volume 4 Electrochemical Materials Science, Plenum Press, New York, 1981.

Sharland, S.M., and P.W. Tasker, *A Mathematical Model of Crevice and Pitting Corrosion-I. The Physical Model*, Corrosion Science, vol. 28, no. 6, pp.603-620, 1988.

Sharland, S.M., *A Mathematical Model of Crevice and Pitting Corrosion-II. The Mathematical Solution*, Corrosion Science, vol. 28, no. 6, pp.621-630, 1988.

Sharland, S.M., C.P. Jackson, and A.J. Diver, *A Finite-Element Model of the Propagation of Corrosion Crevices and Pits*, Corrosion Science, vol. 29, no. 9, pp. 1149-1166, 1989.

Sharland, S.M., *A Mathematical Model of the Initiation of Crevice Corrosion in Metals*, Corrosion Science, vol. 33, no. 2, pp. 183-201, 1992

---

[2] Sharland, S.M., C.P. Jackson, and A.J. Diver, *A Finite-Element Model of the Propagation of Corrosion Crevices and Pits*, Corrosion Science, Vol. 29, no. 9, p. 1153.

Walton, J.C., *Mathematical Modeling of Mass Transport and Chemical Reaction in Crevice and Pitting Corrosion*, Corrosion Science, vol. 30, no. 8/9, pp.915-928, 1990.

Watson, M.K., and J. Postlethwaite, *Numerical Simulation of Crevice Corrosion:The Effect of the Crevice Gap Profile*, Corrosion Science, vol. 32, no. 11, pp. 1253-1262, 1991.

Watson, M.K., and J. Postlethwaite, *Numerical Simulation of Crevice Corrosion of Stainless Steel and Nickel Alloys in Chloride Solutions*, Corrosion, vol. 46, no. 7, pp. 522-530,1990.

Section 3:Fatigue

Definition

Fatigue failure is a general term given to the sudden and catastrophic separation of a machine part into two or more pieces as a result of the application of fluctuating loads or deformations over a period of time.

The major forms of fatigue are:

1. High-cycle fatigue
2. Low-cycle fatigue
3. Crack growth
4. Surface fatigue

Of the various types of fatigue, high-cycle fatigue, low-cycle fatigue, and crack growth.

Physical Process of Fatigue

The fatigue process consists of three stages:

1. Crack initiation phase
2. Subcritical crack propagation
3. Final fracture

Of these stages, most designers are concerned with crack initiation and subcritical crack propagation.

Probability models of fatigue life

Because many of the factors involved are random in nature, the appropriate development of analysis and design methodologies should be probabilistic. Two distributions that have been widely used in fatigue studies are the lognormal and Weibull distributions. Use of the lognormal distribution has been based primarily on arguments of mathematical expediency. However, it has been pointed out by Gumbel(4) that the hazard function for the lognormal model decreases for large values of N. This does not agree with our physical understanding of progressive deterioration resulting from the fatigue process. Nevertheless, the lognormal distribution often seems to provide a "good fit" of cycles to failure data. The Weibull distribution is based on more physical convincing arguments. Moreover, the Weibull distribution is well-suited for certain procedures of statistical extrapolation to large systems(5).

Source:

Fatigue Reliability: Introduction, ASCE, Vol.108, NO. ST1, January,1982

J.A.Collins, Fatigue of Materials in Mechanical Design

Freudenthal, A., Reliability Analysis Based on Time to the First Failure, Aircraft Fatigue, Pergamon Press, Inc., London, England, 1972.

Gumbel, E.J., Parameters in the Distribution of Fatigue Life. Journal of the Engineering Mechanics Division, ASCE, Vol. 89, No. EM5, Oct. 1963.

Paul H. Wirsching, Statistical Summaries of Fatigue Data for Design Purposes, STAR, N83-29731.

3.1 High-Cycle Fatigue

Definition

High-cycle fatigue is associated with lower stress levels and high numbers of cycles to produce fatigue failure. It is typically associated with cycle lives grater than about 10^4 or 10^5 cycles.

Failure Mechanism

The crack initiation period consumes a substantial percentage of the usable fatigue life in high-cycle fatigue problems where stress fluctuations are low at fatigue-critical locations. The crack propagation period is very short compared with the crack growth period.

The classical model (The Basquin Equation):

$$NS^m = C$$

where:

S =stress amplitude, or stress range.
M, C = empirically determined constants which depend on the material and are significantly affected by the environment
N=fatigue life, cycles to failure.

Sources

Fatigue Reliability: Introduction, ASCE, Vol.108, NO. ST1, January,1982

J.A.Collins, Fatigue of Materials in Mechanical Design

3.2 Low-Cycle Fatigue

Definition

Low-cycle fatigue is associated with high stress levels and low number of cycles to produce fatigue failure. It is typically associated with cycle lives from one up to about 10^4 or 10^5 cycles.

Failure Mechanism

When stress fluctuations are high, fatigue cracks initiate quite early and a significant portion of the service life of the component may be spent propagating the crack to critical size. The two phases are of roughly equal importance, in terms of order of magnitude, in low cycle fatigue.

The general model

$$\epsilon_a = \frac{\sigma_f'}{E}(2N)^b + \epsilon_f'(2N)^c$$

where:

ε_a = strain amplitude.
E = modulus of elasticity.
σ'_f =fatigue strength coefficient.
b = fatigue strength exponent.
ε'_f =fatigue ductility coefficient.
c = fatigue ductility exponent.

Note: This model considers elastic strain and plastic strain life separately. The total strain life is the summation of the two.

Source:

Fatigue Reliability: Introduction, ASCE, Vol.108, NO. ST1, January,1982

J.A.Collins, Fatigue of Materials in Mechanical Design

Paul H. Wirsching, Statistical Summaries of Fatigue Data for Design Purposes, STAR, N83-29731.

3.3 Crack growth fatigue

Failure Mechanism

The crack growth rate is given by:

$$\frac{da}{dN} = C(\Delta K)^n$$

$$K = F(a)\, S\sqrt{\pi a}$$

where:

a = crack depth for a surface flaw or half-width for a penetration flaw.
F(a)= finite geometry correction factor which may depend on *a.*
K = stress intensity factor.
S = applied stress.
n, c =experimentally determined constants which depend on the mean cycling stress.

Sources:

Fatigue Reliability: Introduction, ASCE, Vol.108, NO. ST1, January,1982

J.A.Collins, Fatigue of Materials in Mechanical Design

4.1 Thermal Degradation

Definition

Thermal degradation is the deterioration of the functionality or physical properties of a material due to the effects of temperature. The degradation is due solely to the effects of temperature and does not involve with other materials.

Failure Mechanism

The interest in thermal degradation lies in materials that are non-metallic, since thermal influences on metals can result in changes in the grain structure. The material properties of metals possessing different grain structures is well documented. As a result, this examination of thermal degradation will focus primarily on polymers and insulating materials.

In the case of polymers, the two main types of degradation are:

1. Depolymerisation, which is the breaking of the main polymer chain backbone so that at any intermediate stage the products are similar to the parent material in that the monomer units remain distinguishable. The products of the degradation may be monomer, or they may be volatile chain fragments.[1]

2. Substitient reactions result in the attachment of substitients to the backbone of the polymer molecules involved so that the chemical nature of the repeat unit is changed even though the chain structure may remain intact.[2]

In the case of polystyrene, if the chain scission occurs in a polymer molecule without volatilisation, then :[3]

$$P_t = \frac{P_o}{(s+1)}$$

where: P_o *= initial chain length of the polymer*
P_t *= chain length of the polymer after time t*
s *= average number of scissions per molecule*

From this equation the fraction of broken bonds, α, can be found. If the chain scission is random then $\alpha = kt$ where k=rate constant for chain scission. If the chain contains weak and strong links, then $\alpha = \beta + kt$, where β is the fraction of weak links in the molecule.

In practice the approach is to determine the lifetime of polymers using approaches based on

---

[1] Grassie, N., and G. Scott, Polymer Degradation and Stabilisation, Cambridge University Press, Cambridge U.K., 1985, pp. 23-24.

[2] Grassie, N., and G. Scott, Polymer Degradation and Stabilisation, p. 24.

[3] Grassie, N., and G. Scott, Polymer Degradation and Stabilization, pp.28-29.

Arrhenius equations. Gurnay[4] reports that a relationship that accounts for both thermal and radiation degradation on polymers is:

$$a(T,D) = \exp -\frac{E}{R}\left(\frac{1}{T_{ref}} - \frac{1}{T}\right)\left[1 + k \exp\frac{Ex}{R}\left(\frac{1}{T_{ref}} - \frac{1}{T}\right) D^{x}\right]$$

where: E = *activation energy*
R = *gas constant*
T = *absolute temperature polymer environment*
T_{ref} = *reference temperature*
k = *radiation degradation reaction constant*
D = *dose rate*

Note that E, k, and x are empirical constants. The parameter E can be determined from the polymer where radiation is not a problem. Thus, k and x are empirically determined from irradiation data. Gurnay further reports that the majority of polymers studied have been found to have x=1. For cases where x=1, the above relation is simply:

$$a(T,D) = \exp\frac{-E}{R}\left(\frac{1}{T_{ref}} - \frac{1}{T}\right) + kD$$

This relationship is simply the sum of the thermal degradation described by the Arrhenius relationship plus a dose rate component, D, multiplied by a radiation degradation reaction constant, k. In cases where radiation is not significant, the relationship for simple thermal degradation results.

---

[4] Burnay, S.G., *A Practical Model for Prediction of the Lifetime of Elastomeric Seals in Nuclear Environments*, Proceedings from 200th National Meeting of the American Chemical Society, Washington, August 26-31, 1990 (Published in Radiation Effects on Polymers, ACS Symposium Series #475)

Sources

A Review of Equipment Aging Theory and Technology, EPRI Report NP-1558, Project 890-1, Final Report, Electric Power Research Institute, Palo Alto, CA, September 1980.

STS Life Management System Development, SwRI Report No. 06-2148-1A, Project No. 06-2148, Southwest Research Institute, San Antonio, TX, November 30, 1988.

Proceeding of the 200th National Meeting of the American Chemical Society, Washington, August 26-31, 1990.

Grassie, N., and G. Scott, Polymer Degradation and Stabilisation, Cambridge University Press, Cambridge, U.k., 1985.

Schnabel, W., Polymer Degradation, Macmillan Publishing Co., Inc, New York, 1981.

Troitskii, B.B., and L.S. Troitskaya, *Mathematical Models of the Initial Stage of the Thermal Degradation of Poly (vinyl Chloride)*, Journal of Polymer Science:Part A:Polymer Chemistry, vol. 28, pp. 2695-2709, 1990.

Lists of reference papers

1 FATIGUE

1) ASCE Committee on Fatigue and Fracture Reliability, "Fatigue Reliability: Introduction", Journal of the Structure Division, ASCE, Vol. 108, No. ST1, January, 1982.

2) Wirsching, P.H., and Yao, James T.P., "Statistical Methods in Structural Fatigue", Journa of the Structural Division, ASCE, Vol. 96, No. ST6, June, 1970.

3) Wirsching, P.H., "Statistical Summaries of Fatigue Data for Design Purposes", Scientific and Technical Aerospace Reports, Vol. 18, 1983.

4) "A Guide for Fatigue Testing and Statistical Analysis of Fatigue Data", ASTM Special Technical Publication, No. 9I-A, 1963.

5) Huang, X.W., and Hancock, J.W., "A Reliability Analysis of Fatigue Crack Growth Under Random Loading and Life Prediction", Fatigue and Fracture of Engineering Materials and Structures, Vol. 12, No. 3, 1989, pp. 247-248.

6) Tallian, T.E., "Simplified Contact Fatigue Life Prediction Model-Part 1: Review of Published Models", Journal of Tribology, Vol. 114, pp. 207-213, April, 1992.

7) Wirsching, P.H., and Carlson, James R., "Model Identification for Engineering Variables' Journal of the Engineering Mechanics Division, ASCE, Vol. 103, No. EM1, Fabruary, 1977

8) Akyurek, T, and Bilir, O.G., "A Critique on Fatigue Crack Growth Life Estimation Methodologies", Int J Fatigue, Vol. 14, No. 1, pp. 30-34, 1992.

9) Ortiz, K., and Kiremidjian, A.S., "A Stochastic Model for Fatigue Crack Growth Rate Data", Journal of engineering for Industry, Vol. 109, February, 1987.

10) Wagner, G.R., and Mishke, C., "Cycles-to-Failure and Stress-to-Failure Weibull Distribution in Steel Wire Fatigue", Annual Reliability and Maintainability Symposium, Session 7A3, pp. 445-451, 1973.

11) Martin, W.Scott, and Wirsching, P.H., "Fatigue Crack Initiation-Propagation Reliability Model", Journal of Materials in Civil Engineering, Vol. 3, No. 1, February, 1991.

12) Avakov, V.A., and Shomperlen, R.G., "Fatigue Reliability Function", Journal of Vibration, Acoustics, Stress, and Reliability in Design, Vol. 111, October, 1989.

13) Spoormaker, Jan L., "Reliability Prediction of Hairpin-Type Springs", Proceedings, Annual Reliability and Maintainability Symposium, Session 413, pp. 142-147, 1977.

14) Fatigue under Complex Loading. edited by Wetzel, R.M.

2 WEAR

1) Lin, Ji-Yi, and Cheng, H.S., "An Analytical Model for Dynamic Wear", Journal of Tribology Vol. 111, July, 1989.

2) Stolarski, T.A., "A Probabilistic Approach to Wear Prediction", Journal of Physics D, Applied Physics, Vol. 23, pp. 1143-9, September, 1990.

3) Hansen, C.K., and Thyregod, Poul, "Component Lifetime Models Based on Weibull Mixtures and Competing Risks", Quality and Reliability Engineering International, Vol. 8, pp. 325-333, 1992.

3 CORROSION

1) Sharland, S.M., "A Mathematical Model of the Initiation of Crevice Corrosion in Metals", Corrosion Science, Vol. 33, No. 2, pp. 183-201, 1992.

2) Sheikh, A.K., Both, J.K., and Hansen, D.A., "Statistical Modeling of Pitting Corrosion and Pipeline Reliability", Corrosion, Vol. 46, pp. 190-7, March, 1990.

3) Alawi, H., Ragab, A., and Shaban, M., "Corrosion Fatigue Crack Growth of Steels in Various Environments", Journal of Engineering Materials and Technology, Vol. 111, January, 1989.

4) Yamauchi, Kiyoshi, "Analysis of Stress Corrosion Cracking Life Based on Reaction Model", Nuclear Engineering and Design, Vol. 138, No. 3, pp. 239-249, 1992.

5) Nicholls, J.R., and Stephenson, D.J., "A Life Prediction Model for Coatings based on the Statistical Analysis of Hot Salt Corrosion Performance", Corrosion Science, Vol. 33, No. 8, August, 1992.

6) Garud, Y.S., and Mcilree, A.R., "Intergranular Stress Corrosion Cracking Damage Model: An Approach and its Development for Alloy 600 in High-purity Water", Corrosion, Vol. 42, No. 2, February, 1986.

7) Sharland, S.M., and Tasker, P.W., "A Mathematical Model of Crevice and Pitting Corrosion", Corrosion Science, Vol. 28, No. 6, pp. 603-630, 1988.

8) Nakayama, T., and Takano, M., "Application of a slip Dissolution Repassivation Model for Stress Corrosion Cracking of AISI 304 Stainless Steel in a Boiling 42% $MgCI_2$ Solution", Corrosion, Vol. 42, pp. 10-15, January, 1986.

9) Daeubler, M.A. et al, "Modeling of Corrosion Fatigue Crack Initiation under Passive Electrochemical Conditions", Metallurgical Transactions A, Vol. 22A, February, 1991.

10) Turnbull, A., "Review of Corrosion Studies on Aluminium Metal Matrix Composites", British Corrosion Journal, Vol. 27, No. 1, 1992.

4 CREEP

1) Fridley, K., Tang, R.C., and Soltis, L.A., "Creep Behavior Model for Structural Lumber", Journal of Structural Engineering, Vol. 118, No. 8, August, 1992.

2) Gong, Z.L., and Hsu, T.R., "A Constitutive Model for Metals Subjected to Cyclic Creep", Journal of Engineering Materials and Technology, Vol. 113, October, 1991.

3) Kitamura, T., and Ohtani, R., "Creep Life Prediction based on Stochastic Model of Micro structurally Short Crack Growth", Journal of Engineering Materials and Technology, Vol. 111, April, 1989.

4) Krajcinovic, Dusan, and Selvaraj , Sebastine , "Creep Rupture of Metals-An Analytical Model", Journal of Engineering Materials and Technology, Vol. 106, October, 1984.

5) Bayer, R., and Khandros, I., "Model Aids Alloy Life Prediction", Hydrocarbon Processing, Vol. 64, pp. 22-24, January, 1985.

6) Samra, Raed M., "Creep Model for Reinforced Concrete Columns", ACI Structural Journal, Vol. 86, pp. 77-82, 1989.

7) Penny, R.K., and Weber, M.A., "Integrity Assessments of Components in the Creep Range", Journal of Engineering for Gas Turbines and Power, Vol. 113, pp. 574-581, October, 1991.

8) Cohn, M.J., "Remaining Life of High-Energy Piping Systems Using Equivalent Stress", Journal of Pressure Vessel Technology, Vol. 112, pp. 260-265, August, 1990.

Reference books;

1) Haugen, E.B., Probabilistic Mechanical Design.

2) Collins, J.A., Failure of Materials in Mechanical Design.

REPORT DOCUMENTATION PAGE

Form Approved
OMB No. 0704-0188

1. AGENCY USE ONLY (*Leave blank*)	2. REPORT DATE	3. REPORT TYPE AND DATES COVERED
	July 1996	Final Contractor Report

4. TITLE AND SUBTITLE

Compendium of Mechanical Limit-States

5. FUNDING NUMBERS

WU–505–62–10
G–NAG3–1352

6. AUTHOR(S)

Michael Kowal

7. PERFORMING ORGANIZATION NAME(S) AND ADDRESS(ES)

Vanderbilt University
Mechanical Engineering
Nashville, Tennessee 37235

8. PERFORMING ORGANIZATION REPORT NUMBER

E–10246

9. SPONSORING/MONITORING AGENCY NAME(S) AND ADDRESS(ES)

National Aeronautics and Space Administration
Lewis Research Center
Cleveland, Ohio 44135–3191

10. SPONSORING/MONITORING AGENCY REPORT NUMBER

NASA CR–198481

11. SUPPLEMENTARY NOTES

Project Manager, Christos C. Chamis, Structures Division, NASA Lewis Research Center, organization code 5200, (216) 433–3252.

12a. DISTRIBUTION/AVAILABILITY STATEMENT

Unclassified - Unlimited
Subject Category 39

This publication is available from the NASA Center for AeroSpace Information, (301) 621–0390.

12b. DISTRIBUTION CODE

13. ABSTRACT ***(Maximum 200 words)***

A compendium was compiled and is described to provide a diverse set of limit-state relationships for use in demonstrating the application of probabilistic reliability methods to mechanical systems. The different limit-state relationships can be used to analyze the reliability of a candidate mechanical system. In determining the limit-states to be included in the compendium, a comprehensive listing of the possible failure modes that could affect mechanical systems reliability was generated. Previous literature defining mechanical modes of failure was studied, and cited failure modes were included. From this, classifications for failure modes were derived and are described in some detail.

14. SUBJECT TERMS

Reliability; Design methodology; Failure modes; Wear; Corrosion; Fatigue; Thermal degradation

15. NUMBER OF PAGES

56

16. PRICE CODE

A04

17. SECURITY CLASSIFICATION OF REPORT	18. SECURITY CLASSIFICATION OF THIS PAGE	19. SECURITY CLASSIFICATION OF ABSTRACT	20. LIMITATION OF ABSTRACT
Unclassified	Unclassified	Unclassified	